Interplay between the antiferromagnetic spin configuration and the exchange bias effect in $[Pt/Co]_8/CoO/Co_3Pt$ trilayers

Tobias Kosub,[*,†] Denys Makarov,[†] Herbert Schletter, Michael Hietschold, and Manfred Albrecht
Institute of Physics, Chemnitz University of Technology, D-09107 Chemnitz, Germany
(Received 12 August 2011; revised manuscript received 23 September 2011; published 28 December 2011)

The exchange bias effect in $[Pt/Co]_8/CoO/Co_3Pt$ trilayers was studied. The individual reversal of the ferromagnetic layers was analyzed for two cooling configurations in which the magnetic moments were aligned parallel or antiparallel to each other. The exchange bias fields of the ferromagnetic films can be set independently for each configuration, depending on their respective initial magnetization orientations. Still, magnetic coupling between both the $[Pt/Co]_8$ and the Co_3Pt layers is unambiguously observed below the blocking temperature of the antiferromagnetic CoO. This phenomenon is studied by looking at isolated magnetic reversal processes in minor loops and is explained by temporary modifications of the CoO bulk spin structure. Specifically, we suggest that the frozen part of the antiferromagnetic grains is responsible for the coupling.

DOI: 10.1103/PhysRevB.84.214440 PACS number(s): 75.70.−i, 68.65.Ac, 75.50.Ee, 75.60.Ej

I. INTRODUCTION

Magnetism is a collective phenomenon governed by interactions at the atomic scale, resulting in ferromagnetic (F), ferrimagnetic, or antiferromagnetic (AF) arrangement of atomic moments in solids. The most intriguing effects arise when magnetic materials revealing different intrinsic coupling (i.e., F and AF) are brought in contact. One of the prominent examples is the appearance of unidirectional anisotropy as a result of exchange coupling between F and AF layers, first discovered by Meiklejohn and Bean in 1956.[1] This unidirectional anisotropy, also known as exchange bias (EB), leads to the shift (biasing) of the hysteresis loop of the F layer,[2,3] which is of great application relevance for the fabrication of magnetic sensor devices.[4,5]

Although the phenomenon of EB has been studied for more than half a century, many aspects have not yet been explored in detail. Thus, even the origin (bulk or interfacial) of the EB effect is not yet clear. It is generally accepted that EB results from the exchange coupling between F and uncompensated AF spins at the F/AF interface.[6] The microscopic way in which this coupling translates into EB is more controversial, and many models have been proposed.[7–13] Morales *et al.*[14] have recently performed a thorough experimental investigation of the EB effect in an epitaxial trilayer consisting of Ni/FeF_2/permalloy with in-plane easy axis of magnetization in the F layers. It was unambiguously demonstrated—by investigating the EB effect for two cooling configurations, where the F layers are aligned parallel or antiparallel to each other—that the EB effect in this stack has substantial influence on the bulk AF spin configuration.

In this paper, we investigated the EB effect in a polycrystalline $[Pt/Co]_8/CoO/Co_3Pt$ trilayer with an out-of-plane easy axis of magnetization. The magnetic properties of the F layers were optimized to assure a substantial difference in coercive field, thus allowing the preparation of different magnetic states at the interface to the AF CoO. We explore how the reversal of the F1/AF interface affects the bulk AF spin configuration, which can be probed via the EB effect at the other F2/AF interface. This study provides an insight into the influence of the bulk AF spin configuration on the EB effect in the trilayer stack employing a rather thin AF CoO layer. Moreover, we focus on the novel coupling effect between the two F layers across the AF layer, which leads to intriguing changes in the magnetization reversal behavior when comparing single F/AF subsystem minor loops and full loops of the complete F/AF/F trilayer.

II. EXPERIMENTAL DETAILS

A 5-nm-thick Co_3Pt alloy with a perpendicular magnetic easy axis and with a coercive field of ∼600 Oe at 300 K was chosen as a magnetically hard layer. The Co_3Pt films were prepared on thermally oxidized Si(100) wafers with a 100-nm-thick SiO_2 layer by direct current (DC)–magnetron cosputtering of Co and Pt with rates of 0.22 and 0.1 Å/s, respectively. A composition of Co_xPt_{100-x} with $x = 73\pm1$ was determined by Rutherford backscattering spectroscopy. A series of EB Co_3Pt samples was prepared by introducing the samples into the sputter chamber again and depositing an additional 1-nm-thick Co layer, followed by the oxidation of the Co layer at ambient conditions. This procedure also led to an oxidation of the top Co_3Pt surface.[15] Superconducting Quantum Interference Device-Vibrating Sample Magnetometer (SQUID-VSM) measurements of the single CoO layer showed no magnetic signal at room temperature, indicating the complete oxidation of the deposited Co layer. As a magnetically softer layer, a $[Pt(0.77\ nm)/Co(0.28\ nm)]_8$ multilayer film was chosen, revealing a coercivity of 50 Oe at room temperature and full remanence. This film was prepared by alternating DC–magnetron sputtering of Co and Pt species on the CoO/Co_3Pt starting the multilayer stack with a cobalt layer. A 2-nm-thick Pt capping layer was used to protect the samples from oxidation. All metal layers were sputter deposited at room temperature using Ar as a sputter gas at a pressure of 3.5×10^{-3} mbar. In addition to the $[Pt/Co]_8/CoO/Co_3Pt$ trilayer, reference samples consisting of CoO/Co_3Pt and $[Pt/Co]_8/CoO$ bilayers were prepared for comparison.

Structural characterization of the samples was performed using transmission electron microscopy (TEM) in both conventional and high-resolution modes. A cross-sectional TEM image is shown in Fig. 1(a), revealing the three layers of

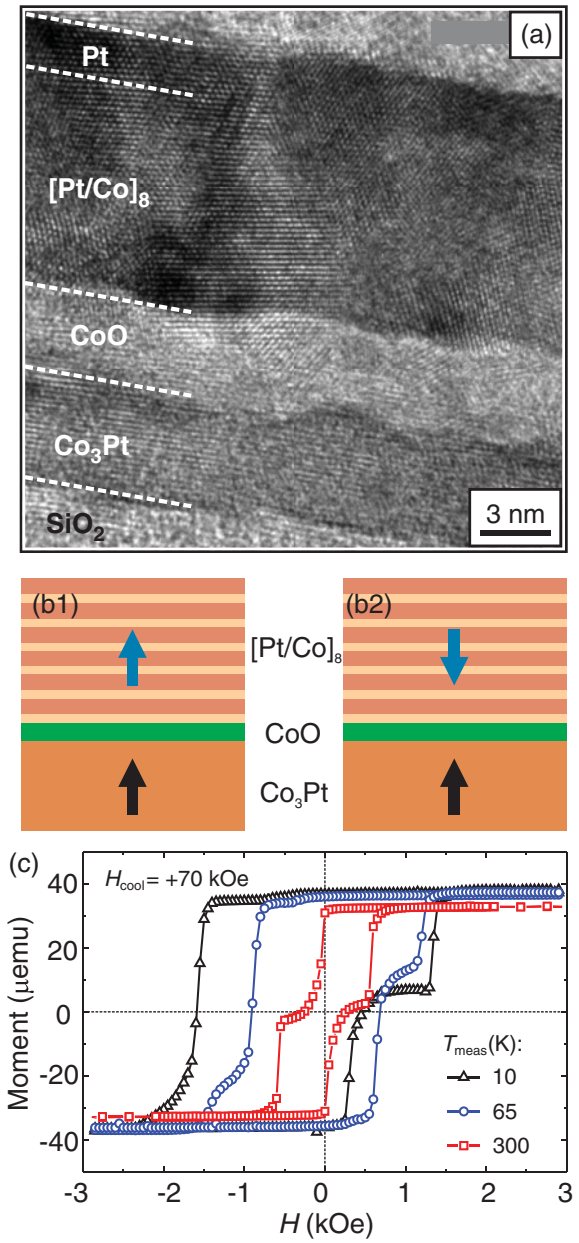

FIG. 1. (Color online) (a) TEM cross-sectional image taken on the $[Pt/Co]_8/CoO/Co_3Pt$ (from top to bottom) trilayer grown on thermally oxidized Si(100). (b) Sketch revealing the magnetic configuration in the F layers in the $[Pt/Co]/_8CoO/Co_3Pt$ stack (b1) after positive saturation and (b2) after exposing the initially saturated layer stack to a reverse magnetic field with a strength larger than H_C of the $[Pt/Co]_8$ layer at room temperature (-400 Oe). (c) Evolution of the hysteresis loop of the $[Pt/Co]_8/CoO/Co_3Pt$ trilayer after cooling in a field of $H_{cool} = +70$ kOe down to the measurement temperature.

the stack. The larger thickness of the CoO layer of $\sim$3 nm compared to its nominal value is related to the oxidation at the top of the Co_3Pt layer[15] and at the first Co layer of $[Pt/Co]_8$ multilayer stack. Analysis of the grain sizes revealed that the CoO layer consists of rather small crystallites with a mean grain size of $\sim$3 nm. However, larger grains with sizes of more than 5 nm were also observed. At the same time, the F films have a grainy film morphology with substantially larger grains of $\sim$10 nm for the Co_3Pt alloy film and $\sim$15 nm for the $[Pt/Co]_8$ multilayer stack.

Magnetic characterization was done in in-plane and out-of-plane geometry of the applied magnetic field using a Quantum Design SQUID-VSM with a maximum field of 70 kOe. The measurements were carried out in the temperature range between 10 and 300 K. Bulk cobalt(II) oxide develops an AF order below its Néel temperature T_N of $\sim$290 K, although a blocking temperature T_B of $\sim$100 K was measured for both CoO/Co_3Pt and $[Pt/Co]_8/CoO$ systems. The used measurement routine included a warming process to 320 K followed by setting the field to $+70$ kOe to saturate both F layers in the same direction. Then, the cooling field H_{cool} was set. With H_{cool} applied, the samples were cooled to the desired measurement temperature T_{meas}, at which hysteresis loops were acquired. After the cooling procedure, the sample was trained to equilibrium (20 cycles with a maximum field of 20 kOe). T_{meas} and H_{cool} were varied to investigate the dependence of the coercivity H_C and the EB field H_{EB} on both parameters.

III. MAGNETIC PROPERTIES OF THE REFERENCE F/AF BILAYERS

A study of the EB effect in a single Co_3Pt layer biased by a thin CoO AF film was recently presented.[15] In agreement with an earlier work by Yamada *et al.*,[16] Co_3Pt alloy films grown on planar amorphous SiO_2 substrates reveal a preferential out-of-plane easy axis of magnetization. The saturation magnetization of the alloy film was estimated to be about $M_{S,Co_3Pt} = (900 \pm 140)$ emu/cm^3, thus resulting in a total moment per unit area of $\sim$405 μemu/cm^2. Being coupled to the CoO layer, the system reveals a shift of magnetic hysteresis loops and an enhancement of the coercivity of the Co_3Pt layer. An interfacial coupling constant J_{EB,Co_3Pt} of 0.19 ergs/cm^2[15] was estimated following the method by O'Grady *et al.*[13] for grainy AF films.

$[Pt/Co]_8$ multilayer films grown on CoO reveal a well-defined, out-of-plane easy axis of magnetization with a saturation magnetization of $M_{S,[Pt/Co]} = (520 \pm 80)$ emu/cm^3. In comparison with the Co_3Pt alloy, the $[Pt/Co]_8$ multilayer stack has a saturation magnetization, which is smaller by almost a factor of 2. However, because the thickness of the $[Pt/Co]_8$ multilayers is about twice as large as that of the Co_3Pt film, the moment per sample area of the two F layers is similar ($\sim$416 μemu/cm^2 for $[Pt/Co]_8$). This is important in the following discussion of the EB effect in the $[Pt/Co]_8/CoO/Co_3Pt$ trilayer stack with opposite orientation of magnetic moments in the F layers. The $[Pt/Co]_8/CoO$ bilayer system exhibits a strong EB effect with an interfacial coupling constant of $J_{EB,Co/Pt} = 0.29$ ergs/cm^2. The latter is in agreement with the study by Maat *et al.*,[17] where a value of 0.25 ergs/cm^2 was estimated for a CoO/[Co/Pt] bilayer.

IV. F/AF SUBSYSTEMS IN THE TRILAYER STACK: MINOR LOOP ANALYSIS

Because of the different coercivities of the hard and soft layer, a double-step hysteresis loop is observed when the complete layer stack is measured at room temperature [Fig. 1(c), square symbols]. This enables the possibility of preparing distinct magnetic states with either parallel or antiparallel

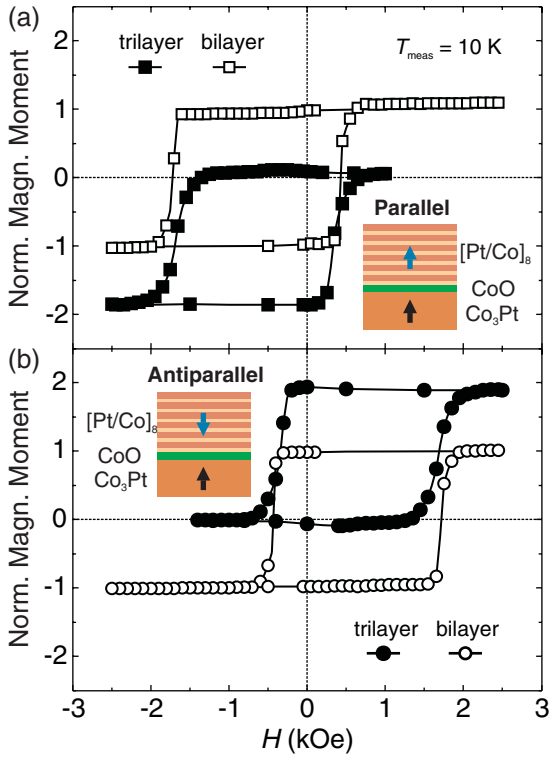

FIG. 2. (Color online) Overlay of the hysteresis loops measured at $T_{meas} = 10$ K comparing trilayer minor $[Pt/Co]_8$ loops (closed symbols) and reference $[Pt/Co]_8/CoO$ bilayer full loops (open symbols) after cooling the samples in a field of (a) $H_{cool} = +400$ Oe and (b) $H_{cool} = -400$ Oe, respectively. The orientations of the magnetic moments in the trilayer stack for the different field cooling processes are also sketched. Minor loops are plotted with respect to the total moment of the fully saturated trilayer stack; therefore, the vertical shifts of the soft layer minor loops are related to the saturated harder Co_3Pt layer.

magnetic orientation of the F layers [Fig. 1(b)] in the samples when cooling below T_B in a certain cooling field. The evolution of the hysteresis loops of the $[Pt/Co]_8/CoO/Co_3Pt$ trilayer with T_{meas} after cooling the stack in a field of +70 kOe [Fig. 1(c)] was recorded. In this case, both F layers stay aligned parallel to each other as sketched in Fig. 1 (b1). Whereas the hysteresis loop measured at room temperature is symmetric, the decrease of the measurement temperature results in an asymmetric hysteresis loop triggered by the onset of the EB effect, resulting (1) in a loop shift and (2) different magnetization reversal mechanisms for the ascending and descending branches for the individual F layers.[18,19] Under these conditions (parallel cooling alignment of the two F layers), the analysis of the coercive and EB fields for different T_{meas} and H_{cool} revealed that the H_C and H_{EB} values of the softer F layers in the trilayer stack are quite similar to those values of the reference bilayer sample. In Fig. 2, the full hysteresis loop of the $[Pt/Co]_8/CoO$ reference bilayer system is compared to the $[Pt/Co]_8$ reversal in the trilayer stack. For the latter, only a *minor* loop of the $[Pt/Co]_8$ reversal was measured. Thus, in this study, the orientation of the magnetic moment of Co_3Pt was fixed and only the magnetization reversal of the softer $[Pt/Co]_8$ layer was followed. This measurement scheme is mimicking conventional investigation of the EB effect in F/AF bilayers. The matching of trilayer minor hysteresis loops and bilayer hysteresis loops [Fig. 2(a)] confirms that in the parallel configuration, the hard Co_3Pt layer at the opposite interface does not notably influence the EB field and coercivity of the soft $[Pt/Co]_8$ layer.

However, as the CoO/Co_3Pt and $[Pt/Co]_8/CoO$ interfaces were in the same magnetic state [Fig. 1 (b1)] after the field cooling procedure, the presented data do not answer the question whether the two interfaces are dependent or independent of each other. Therefore, a different cooling state with antiparallel orientation of the magnetic moments of the two F layers [Fig. 1 (b2)] was realized by cooling the sample in a field of $H_{cool} = -400$ Oe after initial saturation of both F layers in the same direction in a field of +70 kOe. The applied reverse magnetic field of −400 Oe does not influence the magnetic state of the Co_3Pt layer.[15]

Comparing the $[Pt/Co]_8$ minor loops measured after cooling in such an antiparallel configuration [Fig. 2(b), filled circles] to those measured after cooling in a parallel configuration [Fig. 2(a), filled squares] clearly proves that the EB effect of the $[Pt/Co]_8/CoO$ bilayer is independent of the relative arrangement of the two F layers: the minor loops appear unaffected apart from the expected sign change of the loop shift. A similar behavior was observed while measuring at various temperatures below the blocking temperature. Thus, analysis of the minor loops of $[Pt/Co]_8$ suggests that the EB effect is of interfacial origin and that the bulk AF spin configuration plays a negligible role when using a strong antiferromagnet. This finding is different from that in the work of Morales *et al.*,[14] where a weak AF material was used, which might explain the altered bulk AF spin configuration.

Furthermore, the identical $[Pt/Co]_8$ minor loops for the two cooling configurations show that a possible magnetic coupling between the two F layers (i.e., orange peel coupling[20] and Ruderman-Kittel-Kasuya-Yosida-type coupling[21]), preferring one relative alignment over the other, is of minor importance, because no change in the loop shift was observed.

In Fig. 3, a summary of the measured H_C and H_{EB} fields of the $[Pt/Co]_8$ layer [Fig. 3(a)] and Co_3Pt layer [Fig. 3(b)] in the trilayer stack is given. Whereas the values for $[Pt/Co]_8$ could be obtained from the minor loop measurements [Fig. 2, closed symbols], we had to evaluate both antiparallel [Fig. 3(c)] and parallel [Fig. 3(d)] cooling configurations to determine the left and right coercive fields of the Co_3Pt layer. The H_C and H_{EB} values for the Co_3Pt layer in the stack show good agreement with those of the bilayer reference samples.[15]

V. F/AF/F TRILAYER STACK: FULL LOOP ANALYSIS

As already pointed out, when looking at the isolated reversal of the $[Pt/Co]_8$ layer (minor loops, black curves in Fig. 4), no dependence on the cooling state is found apart from the expected sign change of the loop shift. However, even though the EB can be set independently for each F/AF interface and commensurately with respect to the bilayer reference systems, the two present EB subsystems are not magnetically decoupled from each other, as becomes evident when analyzing the full hysteresis loops [Fig. 4, red (gray) curves]. When measuring *full* loops of the trilayer stack, which

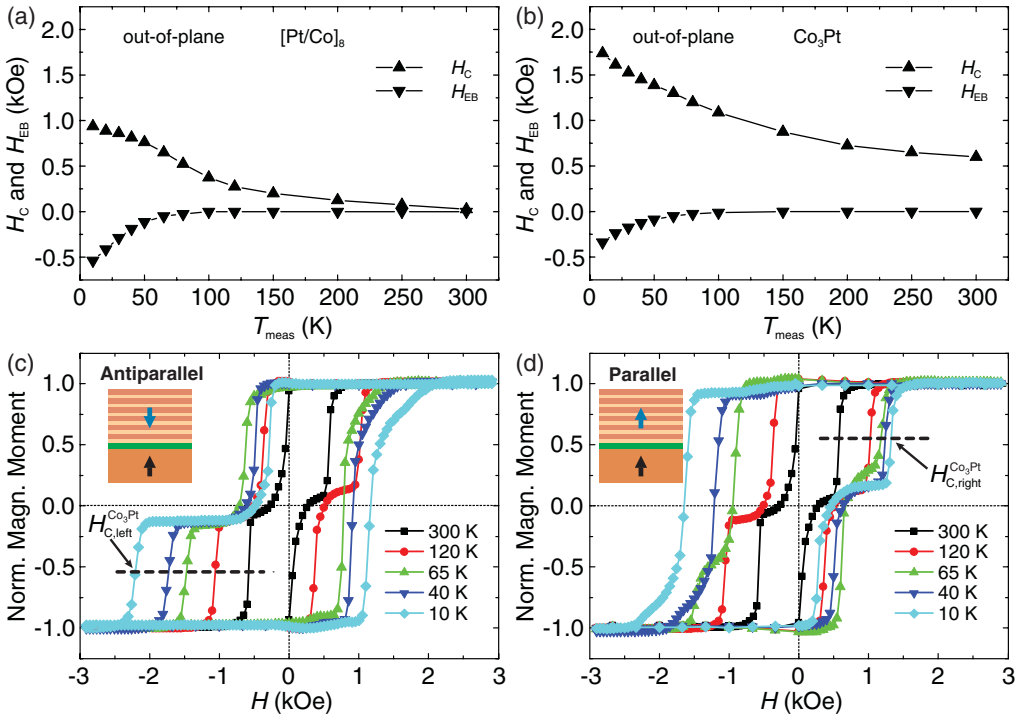

FIG. 3. (Color online) Temperature dependences of the coercive (upward triangles) and EB fields (downward triangles) of each of the F layers in the trilayer stack: (a) $[Pt/Co]_8$ and (b) Co_3Pt. Hysteresis loops measured at various temperatures showing the evaluation method of the (c) left (after antiparallel cooling) and (d) right (after parallel cooling) coercive fields of the Co_3Pt layer. The Co_3Pt coercive fields are the ones at which the hysteresis loop crosses the dashed line, which represents no total Co_3Pt moment at simultaneous $[Pt/Co]_8$ saturation. The presented coercivity is defined as $H_C = \frac{1}{2}(H_{C,right} - H_{C,left})$.

now includes the reversal of the harder Co_3Pt layer, the reversal of the $[Pt/Co]_8$ layer is substantially altered: (1) there is a clear merging of the hysteresis loop branches of the soft and hard layers, and (2) the descending branch measured after parallel cooling [Fig. 4(a)] and the ascending branch measured after antiparallel cooling [Fig. 4(b)] reveal that the reversal of the softer $[Pt/Co]_8$ happens in a substantially smaller field than in the corresponding *minor* loops. These drastic effects, which become even more obvious by looking at the first derivative dm/dH of the corresponding loops [Figs. 4(c) and 4(d)], can only be caused by a modification of the bulk CoO spin structure, because this is the connecting element between the two F-AF subsystems.

The derivative of the descending branch of the full hysteresis loop measured after cooling in parallel configuration is shown in Fig. 4(c). It supports two intriguing details of the present F-AF-F coupling mechanism. First, the derivative reveals the presence of two peaks, of which the one at the low field region is related to the reversal of the soft $[Pt/Co]_8$ film and a part of the Co_3Pt film. While the nucleation field (i.e., the onset of magnetization reversal) of $\sim$1.0 kOe remains rather similar for the $[Pt/Co]_8$ film when comparing minor and full loops, the average switching field expressed by the dm/dH peak position has changed from approximately 1.7 kOe (minor loop) to 1.6 kOe (full loop). This change indicates that the reversal of $[Pt/Co]_8$ occurs earlier in the full loop. Second, the derivative of the full loop is *lower* than that of the minor loop for applied fields between 1.7 and 2.0 kOe. This is suggestive for the mutual nature of the present F-AF-F coupling mechanism: If, in contrast, only the reversal of the softer $[Pt/Co]_8$ caused a simultaneous switching of parts of the harder Co_3Pt, we would expect a derivative that is always *equal to or greater than* that of the $[Pt/Co]_8$ minor loop.

The mutual stimulation for magnetization reversal between the two F layers is even more pronounced on the ascending branch of the hysteresis loop measured after antiparallel cooling [Figs. 4(b) and 4(d)]. Here, although the nucleation field remains unchanged, the magnetization reversal commences in a much lower field. Similar data are given in Fig. 5 for measurements done at 40 and 65 K. For higher temperatures ($T_{meas} > T_B$), evidence of F-AF-F coupling vanishes, which means that the dm/dH curves of the trilayer full loops track exactly the ones for the corresponding $[Pt/Co]_8$ minor loops (not shown).

This behavior can be explained in the following way: The AF layer consists of magnetically exchange-decoupled CoO grains,[13,15] the interfacial AF/F coupling energy is J_{EB}, and the anisotropy energy of the AF grains can be expressed by the product $K_{AF} \cdot t_{AF}$ (t_{AF}: thickness of the AF layer).[9,22] CoO is a rather strong AF with a high anisotropy constant K_{AF} of 29×10^7 ergs/cm^3.[23] However, the mean size of the CoO grains is $\sim$3 nm, resulting in a reduced thermal stability. The magnetic spin configuration of such an AF grain can be altered if the torque induced by a strongly exchange-coupled F layer is sufficient (J_{EB} comparable to or greater than $K_{AF} \cdot t_{AF}$), which was proposed by Meiklejohn and Bean.[9,22,24] In a realistic sample, the grain size distribution leads to finite widths of the distributions of J_{EB} and $K_{AF} \cdot t_{AF}$ for a given T_{meas}. Therefore,

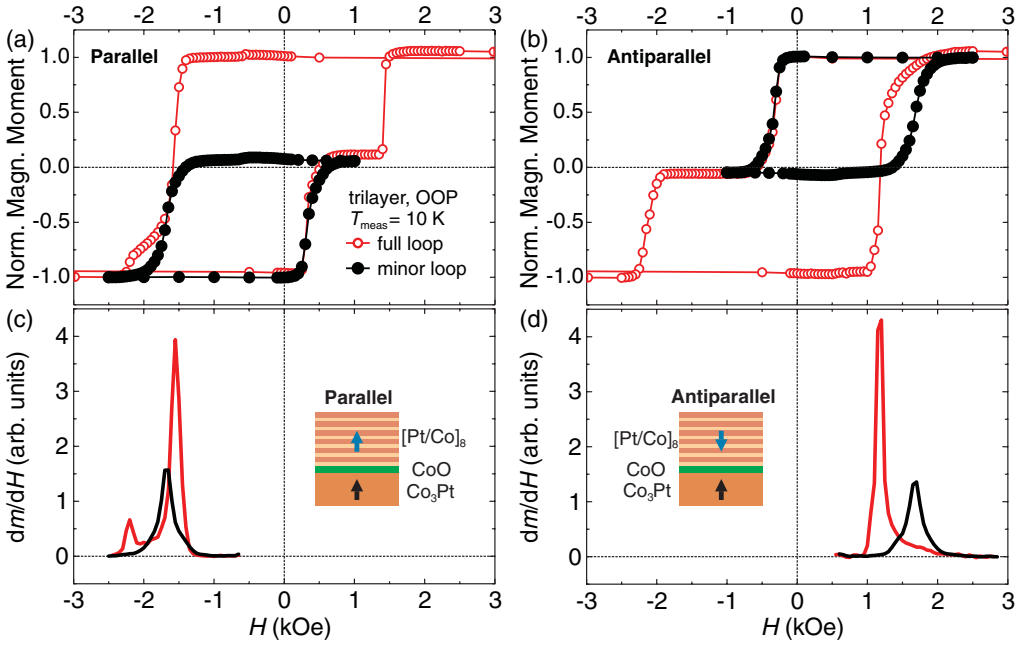

FIG. 4. (Color online) Hysteresis loops measured at $T_{meas} = 10$ K of the $[Pt/Co]_8/CoO/Co_3Pt$ trilayer after cooling in (a) parallel ($H_{cool} = +400$ Oe) and (b) antiparallel ($H_{cool} = -400$ Oe) configurations. Full loops are presented as open symbols, and $[Pt/Co]_8$ minor loops are shown as filled symbols. The $[Pt/Co]_8$ minor loops were measured while going to negative (positive) saturation from the plateau region of the hysteresis loop at +1.0 (−1.0) kOe and back. The first derivatives dm/dH of the outer full and minor loop branches are presented in panels (c) and (d). The inset images show the cooling configuration.

at a certain measurement temperature $T_{meas} < T_B$, both cases with $J_{EB} < K_{AF} \cdot t_{AF}$ (frozen spin configuration) and $J_{EB} > K_{AF} \cdot t_{AF}$ (rotatable AF net moment) are expected. Those AF

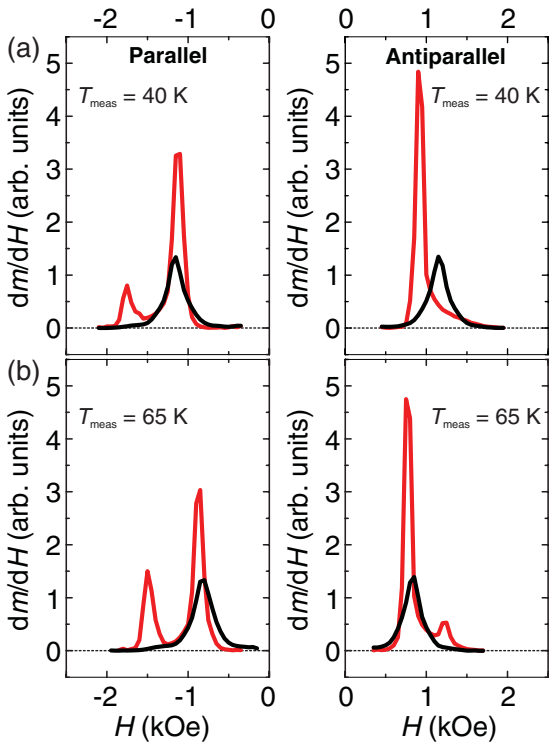

FIG. 5. (Color online) Derivatives of merged hysteresis loop branches and respective minor loop branches as shown in Figs. 4(c) and 4(d) but for temperatures of (a) 40 K and (b) 65 K.

grains with a rotatable net moment cannot contribute to the loop shift, which is created by the AF grains with a frozen spin structure.[6] To understand the F-AF-F coupling, both shares of AF grains (rotatable net moment and frozen structure) have to be considered individually.

First, the grains with rotatable net moments are considered. By changing the magnetic configuration of the trilayer stack at T_{meas}, we introduce frustrations in the bulk AF spin configuration, affecting the magnetization reversal behavior of both F layers. However, by looking at the minor loops shown in Figs. 4(a) and 4(b) (black curves), we see that they are identical despite experiencing the Co_3Pt layer in its cooling state [Fig. 4(b)] and antiparallel to its cooling state [Fig. 4(a)]. Therefore, the spin structure in the AF grains with rotatable net moments is only altered in a way that does not significantly affect the opposing F layer—e.g., only in the interfacial regions. This finding is in agreement with the recent work by Xu *et al.*[25] where F/AF subsystems in a trilayer stack with an in-plane easy axis of magnetization are found to be decoupled when the thickness of the FeMn AF layer is above a critical thickness of a few nanometers corresponding to the two interfacial layers influenced by EB. The conclusions regarding AF grains with rotatable net moments make it appear rather unlikely that they can substantially influence the magnetization reversal of individual F layers in the trilayer stack.

Thus, we focus now on the AF grains with a frozen spin structure. Those grains have maintained their net moment throughout the training procedure (cycling the field 20 times with a maximum field of 20 kOe). Still, when an adjacent F domain is reversed, the AF spin structure is exposed to the same magnetic torque given by the AF/F exchange coupling, which leads to the flip of the net moment in the AF grains with

rotatable moments. As, however, the rigid (frozen) AF spin structure cannot absorb this torque in the form of flipped spins, a collective disturbance of the spin structure is expected.[26] This disturbance leads to a temporary reduction of the EB effect on both AF/F interfaces. This event allows the reversal of the F layers in a weaker external field compared to the one needed with the AF layer undisturbed. Therefore, the observed, mutually stimulated reversal of the two F layers in trilayer full hysteresis loops originates from the frozen part of the AF spin structure. If there are no AF grains with a frozen spin structure above the blocking temperature, the F-AF-F coupling is expected to vanish as observed experimentally.

VI. CONCLUSIONS

We explored the EB effect in a polycrystalline $[Pt/Co]_8/CoO/Co_3Pt$ trilayer stack with $[Pt/Co]_8$ and Co_3Pt layers possessing out-of-plane easy axes of magnetization. The analysis of the magnetization reversal process of the trilayer after cooling in either parallel or antiparallel orientation of the magnetic moments of the two F layers clearly revealed the occurrence of a coupled magnetization reversal of the two F layers, which is mediated by a temporary disturbance of the spin configuration in the frozen AF grains below. The performed study suggests that the bulk part of the AF grains in EB systems is influenced by the magnetization reversal of the F layer. This effect cannot be observed in classic F/AF bilayers. In contrast, when a F/AF/F trilayer stack is investigated, the second ferromagnet at the opposite interface of the thin AF layer acts as a sensor that allows one to observe the modification of the AF volume spin arrangement induced by the reversal event of a F layer.

The magnetic F-AF-F coupling discussed here leads to cross talk between F layers through the frozen grains of the AF material via a propagating magnetic excitation. This propagation experiences rather low damping as no absorption of the magnetic torque takes place.[26] At the same time, the charge current resistance of the insulating CoO is rather high. Hence, such F-AF-F systems are potentially interesting for the generation of pure spin currents.[27,28]

ACKNOWLEDGMENTS

The authors thank C. Schubert and C. Brombacher for fruitful discussions, M. Daniel and G. Beddies for RBS data analysis and B. Mainz for TEM sample preparation.

*t.kosub@ifw-dresden.de

†Present address: Institute for Integrative Nanosciences, IFW Dresden, D-01069 Dresden, Germany.

[1] W. H. Meiklejohn and C. P. Bean, Phys. Rev. **102**, 1413 (1956).

[2] A. E. Berkowitz and K. Takano, J. Magn. Magn. Mater. **200**, 552 (1999).

[3] J. Nogués and I. K. Schuller, J. Magn. Magn. Mater. **192**, 203 (1999).

[4] B. Dieny, P. Humbert, V. S. Speriosu, S. Metin, B. A. Gurney, P. Baumgart, and H. Lefakis, Phys. Rev. B **45**, 806 (1992).

[5] J. S. Moodera, L. R. Kinder, T. M. Wong, and R. Meservey, Phys. Rev. Lett. **74**, 3273 (1995).

[6] F. Radu and H. Zabel, Springer Tracts Mod. Phys. **227**, 97 (2007).

[7] D. Mauri, H. C. Siegmann, P. S. Bagus, and E. Kay, J. Appl. Phys. **62**, 3047 (1987).

[8] A. P. Malozemoff, Phys. Rev. B **35**, 3679 (1987).

[9] M. D. Stiles and R. D. McMichael, Phys. Rev. B **60**, 12950 (1999).

[10] U. Nowak, K. D. Usadel, J. Keller, P. Miltényi, B. Beschoten, and G. Güntherodt, Phys. Rev. B **66**, 014430 (2002).

[11] D. Suess, M. Kirschner, T. Schrefl, J. Fidler, R. L. Stamps, and J.-V. Kim, Phys. Rev. B **67**, 054419 (2003).

[12] J. Nogués, J. Sort, V. Langlais, V. Skumryev, S. Suriñach, J. S. Muñoz, and M. D. Baró, Phys. Rep. **422**, 65 (2005).

[13] K. O'Grady, L. E. Fernandez-Outon, and G. Vallejo-Fernandez, J. Magn. Magn. Mater. **322**, 883 (2010).

[14] R. Morales, Z.-P. Li, J. Olamit, K. Liu, J. M. Alameda, and I. K. Schuller, Phys. Rev. Lett. **102**, 097201 (2009).

[15] T. Kosub, C. Schubert, H. Schletter, M. Daniel, M. Hietschold, V. Neu, M. Maret, D. Makarov, and M. Albrecht, J. Phys. D Appl. Phys. **44**, 015002 (2011).

[16] Y. Yamada, W. P. Van Drent, E. N. Abarra, and T. Suzuki, J. Appl. Phys. **83**, 6527 (1998).

[17] S. Maat, K. Takano, S. S. P. Parkin, and E. E. Fullerton, Phys. Rev. Lett. **87**, 087202 (2001).

[18] M. R. Fitzsimmons, P. Yashar, C. Leighton, I. K. Schuller, J. Nogués, C. F. Majkrzak, and J. A. Dura, Phys. Rev. Lett. **84**, 3986 (2000).

[19] J. Camarero, J. Sort, A. Hoffmann, J. M. García-Martín, B. Dieny, R. Miranda, and J. Nogués, Phys. Rev. Lett. **95**, 057204 (2005).

[20] J. Moritz, F. Garcia, J. C. Toussaint, B. Dieny, and J. P. Nozières, Europhys. Lett. **65**, 123 (2004).

[21] S. S. P. Parkin, N. More, and K. P. Roche, Phys. Rev. Lett. **64**, 2304 (1990).

[22] M. G. Blamire, M. Ali, C.-W. Leung, C. H. Marrows, and B. J. Hickey, Phys. Rev. Lett. **98**, 217202 (2007).

[23] J. Kanamori, Prog. Theor. Phys. **17**, 177 (1957); **17**, 197 (1957).

[24] W. H. Meiklejohn and C. P. Bean, Phys. Rev. **105**, 904 (1957).

[25] Y. Xu, Q. Ma, J. W. Cai, and L. Sun, Phys. Rev. B **84**, 054453 (2011).

[26] K. H. Michel and F. Schwabl, Z. Physik **238**, 264 (1970).

[27] S. A. Wolf, D. D. Awschalom, R. A. Buhrman, J. M. Daughton, S. von Molnár, M. L. Roukes, A. Y. Chtchelkanova, and D. M. Treger, Science **294**, 1488 (2001).

[28] A. Hoffmann, Phys. Stat. Sol. **4**, 4236 (2007).